SUB-0.05° PRECISION OPTOFLUIDIC DUAL-AXIS INCLINOMETER

Sebastian Wahl, Frédéric Marty, Nicolas Pavy, Bruno Mercier, Dan E.Angelescu
Université Paris-Est, ESIEE Paris / ESYCOM Lab, Noisy-le-Grand, FRANCE

ABSTRACT

This paper details a low-power bi-axial miniaturized inclinometer based on a mobile mass (spherical ball or fluidic droplet) positioned on a precision curved surface that is generated using a novel MEMS process. The detection of the mobile mass was implemented through an external optical system, using a quadrant photodetector. Nanotopography and chemical treatment of the curved surface have been implemented to increase accuracy when using a fluidic mobile mass, by tailoring wetting properties and minimizing contact angle hysteresis. We achieve a range of ±1° with a true linear bi-axial measurement of precision better than 0.05°.

INTRODUCTION

Inclinometers have a large array of applications in multiple industrial fields including automotive, aerospace, mechanical and civil engineering. Certain applications, such as long-term continuous monitoring of major civil engineering works (large buildings, bridge pillars, dams) require autonomous sensors embedded within structures and responding to a combination of low measurement range (±2° typical), high accuracy (0.01°), low cost, low power consumption (<mW), small size, and reduced maintenance. Bi-axial measurements are often necessary, which often requires using two single-axis inclinometers, implying increase in power consumption, cost and logistics.

There have been numerous attempts at developing accurate inclinometers across different measurement ranges. Many miniaturized inclinometer concepts implement variations of the pendulum concept with various techniques of detecting changes in the pendulum state: resistive [1], capacitive [2], electrolytic [3] magnetic [4], optical [5], thermal [6] and photoelectric [7,8,9]. Commercial systems based on dual-axis MEMS accelerometers can deliver accuracies of order 0.1° over a full 180° range, albeit with relatively high power consumption (>30mW) [10]. Currently, the only systems that can achieve the satisfactory combination of the range and accuracy requirements for civil engineering monitoring are classical pendulum inclinometers (force balance tilt sensors), yet they do not satisfy the cost, size, and power consumption criteria.

We present a low-power bi-axial miniaturized inclinometer based on a mobile mass (spherical ball or fluidic droplet) positioned on a precision curved surface that is generated using a novel MEMS process and that does satisfy the above mentioned criteria of cost, size and power consumption. The detection of the mobile mass is implemented through an external optical system using a quadrant photodetector and a LED for shadow tracking of the mobile mass. Nanotopography and chemical treatment of the curved surface have been implemented to increase accuracy when using a fluidic mobile mass, by tailoring wetting properties and minimizing contact angle hysteresis.

We demonstrate the concept using a prototype based on a silicon membrane and a high-precision steel sphere as a mobile mass. We achieve a measurement range of ±1° with a true linear bi-axial measurement of precision better than 0.05°. The use of a nanostructured and chemically treated silicon membrane in combination with a mercury droplet resulted in even better precisions but also suffered from hysteresis effects.

OPERATION PRINCIPLE

Our inclinometer is composed of three main components: a sensitive element, a deflected silicon membrane of perfectly controlled geometry, and an optical detection system (Figure 1).

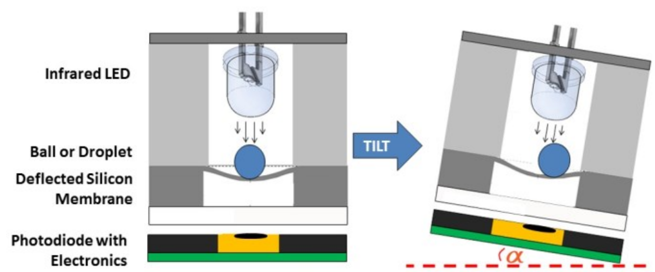

Figure 1: Schematic view of our inclinometer respectively in a non-tilted (left) and tilted state (right).

The sensitive element consists either of a metallic high-precision ball (with very low surface roughness and good sphericity) or alternatively a fluidic mercury droplet which eliminates imprecisions due to roughness but introduces other considerations such as contact angle hysteresis. We attempted to limit hysteresis by rendering the surface superhydrophobic using combined nano-structuring and chemical treatments.

The mobile mass is placed on the silicon membrane which is initially deflected due to the encapsulation of a vacuum cavity. The deflection of the membrane can be controlled by adjusting its geometry.

The shadow projected by the mobile mass is detected optically using a quadrant photodetector and a light source. The perfect control of the deflection and the very low membrane and mobile mass roughness enable accurate prediction of mobile mass displacement when the sensor is tilted and thus accurate tilt angle calculations.

FABRICATION

An aluminium thin film is photolithographically patterned on a 400µm silicon wafer to obtain circular openings that will be used as Deep Reactive Ion Etching (DRIE) etching masks for the silicon (Figure 2). The etch depth is chosen so as to preserve the desired membrane thickness. The geometric parameters of the membrane (diameter and thickness) directly influence its deflection profile and thus the overall measurement range of the inclinometer. After DRIE etching and aluminium removal, a second optional photolithography and cryogenic DRIE step can be performed on the opposite side of the wafer, in order to provide nano-scale topography. An additional 100nm thick fluoropolymer layer is deposited in a C_4F_8 plasma reactor, which results in a superhydrophobic surface as reported earlier (Figure 3) [11]. These additional steps are only performed when a fluidic droplet is used as a mobile mass in order to limit the contact between membrane and droplet. A last step involves the anodic bonding of a 500µm thick glass wafer to the silicon wafer in order to form a cavity in which vacuum is encapsulated. This pressure difference between the vacuumed cavity and the external environment causes the deflection of the silicon membrane in a perfectly controlled and reproducible way.

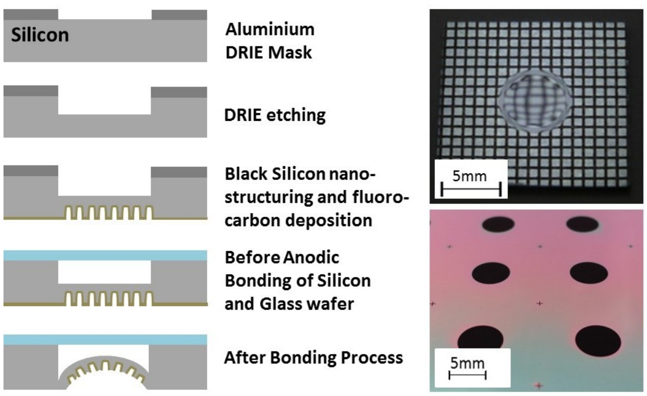

Figure 2: Left: Fabrication process of the nanostructured and chemically treated curved silicon membrane. Top Inset: Reflection of square grid seen in deflected unstructured membrane. Bottom Inset: Array of nanostructured membranes.

The mobile mass displacement is detected using an external optical system consisting of an infrared LED and a quadrant photodetector, which essentially enables the shadow tracking of the mobile mass displacement on the deflected silicon membrane. The wavelength of the infrared LED was chosen at 1070nm which ensures on one hand low silicon absorption and high spectral response of the quadrant photodetector to get an accurate signal of the shadow displacement.

We machined a mechanical aluminium packaging which integrated the quadrant photodetector with conditioning electronics (from First Sensor), the infrared LED (from Thorlabs), the deflected silicon membrane and the mobile mass.

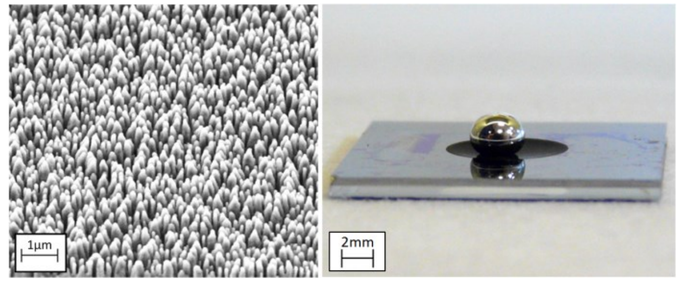

Figure 3: Left: Black-silicon nanostructuring of the membrane using a cryogenic RIE process. Right: Mercury droplet on Black Silicon membrane with fluoropolymer thin film.

DESIGN CONSIDERATIONS

Different parameters need to be taken into account for an optimal sensor design: silicon membrane geometry (diameter and thickness), characteristics of the mobile mass (size, surface roughness and sphericity) and size of the photodetector's sensitive area.

The deflection profile of the silicon membrane (for small scale deflections) can be described mathematically by the equation of a circular thin homogeneous isotropic clamped plate, subjected to a known uniform differential pressure as follows with axisymmetric boundary conditions[12]:

$$y(r) = -y_c + \frac{M_c r^2}{2D(1+\nu)} + LT_y \tag{1}$$

where r is the radial position coordinate, $y(r)$ is the deflection corresponding to r, $y_c = qa^4/64D$ is the maximal center deflection, q is the pressure difference, a is the membrane radius, $M_c = qa^2/[16(1+\upsilon)]$ is the moment at the membrane center, $D = E_y t^3/[12(1-\upsilon^2)]$ is the plate constant, E_y being the Young Modulus, υ the Poisson's ratio, t is the membrane thickness, and $LT_y = -qr^4/64D$ is the loading term. This known deflection profile enables us to find the membrane inflection point r_{inf}, which is the maximal point of equilibrium for the mobile mass, and the associated maximal angle detectable by the sensor Θ_{max}:

$$r_{\inf} = \sqrt{\frac{a^2}{3}} = a\frac{\sqrt{3}}{3} \tag{2}$$

$$\theta_{\max} = \arctan(\frac{\sqrt{3}}{72}\frac{qa^3}{D}) = \arctan(1.54\frac{y_c}{a}) \tag{3}$$

When the ratio y_c/t is greater than 0.3, the small scale deflection equation doesn't apply anymore, and large scale deflection calculations have to be performed. However, the normalized profile remaining largely identical[13], equations 2-3 still hold but a larger effective thickness corresponding to the same maximal center deflection needs to be used.

The characteristics of the mobile mass in terms of size, surface roughness and sphericity are also an important point for the sensor performance. In order to be detectable, the mobile mass shadow must always be in contact with the four detector photoquadrants. The smaller the mobile mass, the sooner the shadow leaves the detector area, and the smaller the measurable tilt angle range. The optimal mobile mass radius needs to correspond to the distance from center to inflexion point, for the quadrant photodetector to be able to detect the position over the full measurement range. The mobile mass should be as spherical and as smooth as possible to ensure repeatable and predictable displacements. Surface roughness of the membrane is nearly atomic, corresponding to that of a high-quality polished silicon wafer.

The size of the photodetector's sensitive area must enable a measurement of mobile mass maximal displacement in order to be able to measure the full sensor tilt range. Thus its diameter must correspond to at least two times the distance from the center to the membrane inflection point.

A first set of circular membranes of 2.83mm radius and 20µm thickness have been produced, with a maximal center deflection of 89,8µm measured by interferometry (in good correlation with large scale deflection calculations done with the ANSYS software package predicting 90,4µm). The inflexion point of these membranes has been calculated to be 1.63mm (from equation 2), which implies the use of a mobile mass with a comparable radius and a maximal measurable tilt angle of 2.4° (computed from equation 3 with an effective membrane thickness of 48µm).

A second set of membranes with nanostructuring and fluorocarbon deposition has been produced with a residual membrane thickness of approximatively 16µm (Figure 3).

EXPERIMENTAL SETUP

The inclinometer has been tested for low tilt angles via a dedicated experimental setup platform described in Figure 4. It consists of a common plate on which the prototype and two uni-axial reference inclinometers (Schaevitz LSOP/LSOC-3 from Sherborne Sensors Limited [14]) are mounted. These reference inclinometers are force balance sensors, with a measurement range of ±3° and a precision of ±0.0006°.

The tilt of the entire platform can be uni-axially changed by adjusting a set of screws drilled through the common plate and in contact with the ground.

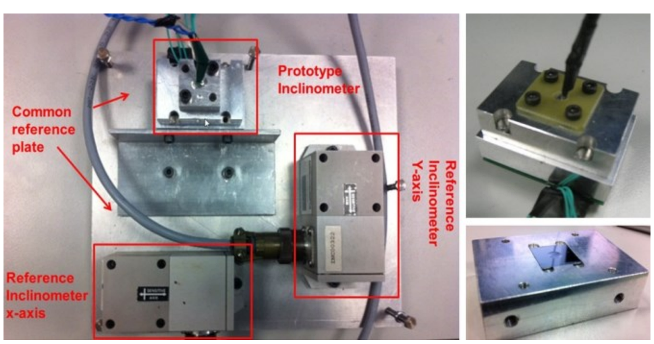

Figure 4: Left: Experimental set-up for inclinometer characterization. Top Inset: Picture of the complete prototype (5.5cm×4cm×3.5cm). Bottom Inset: Membrane holder.

The prototype inclinometer needs to be calibrated before beginning a measurement campaign in order to precisely align the prototype's zero tilt position with the zero position measured by the reference sensors. Any residual offset between the measurements of the reference sensors and the ones of the prototype is removed in software. A dedicated LabWindows software has been programmed that enables simultaneous visualization and acquisition of datapoints from the reference and prototype inclinometers through a National Instruments acquisition card (NI USB 62-59).

RESULTS

Different sets of experiments have been conducted with the two type of membranes previously described in the fabrication section.

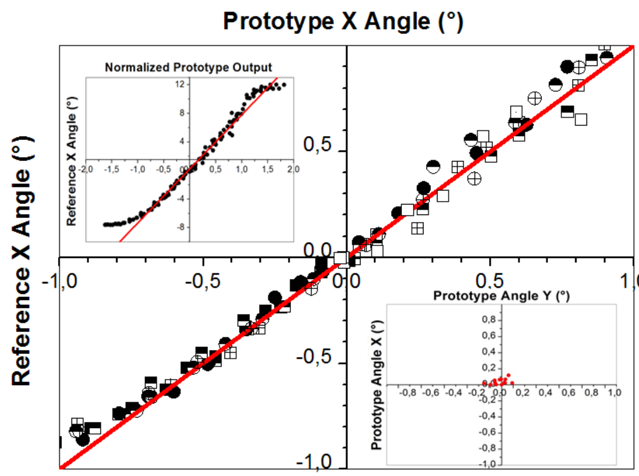

Figure 5: Experimental results of the unstructured membrane. Main graph: Plot showing good correlation between prototype and reference inclinometer measurements over the ±1° linear range. No sign of hysteresis (ascending sweeps with circles, descending with rectangles). Top left Inset: Normalized output of the prototype. Flattening outside the linear range is due to mobile mass shadow leaving center of quadrant detector. Linear fit to obtain calibration coefficient of 7,6/°. Bottom right Inset: Repeatability test following large angle tilt (>10°) showing standard deviation: y=0,033°, x=0,063°

A first measurement campaign (Figure 5) has been performed with an untreated silicon membrane and a 2.38mm diameter high precision steel ball (surface roughness variations of 0,025µm and sphericity error of 2.5µm). The prototype output data has been normalized by dividing the axis-sensitive voltage outputs of the photodiode (left minus right, top minus bottom) by its voltage sum. A linear fit has been performed on experimental data to obtain a slope calibration coefficient. The offset has been measured at 0° inclination and removed prior to plotting the data. The prototype output shows a ±1° linear range with good correlation to the reference inclinometer measurements. Imprecision is introduced through random surface roughness distribution and sphericity errors of the mobile mass. To estimate the precision of the sensor, repeatability tests have been performed. Repeatability tests have been done by placing the prototype in a no-tilt position and realizing repeated large angle tilts (>10°) and coming back to zero. Results show standard deviations of respectively 0.033° and 0.063° in y and x direction.

A second measurement campaign has been performed with a nanostructured and chemically treated silicon membrane and a mercury droplet of approximatively 2mm. The results are illustrated in Figure 6 and clearly show significant hysteresis effects between ascending and descending measurements (data points show a linear progression but are shifted by an offset dependent on the direction of angle change). Repeatability tests show improved standard deviation results of respectively 0.024°

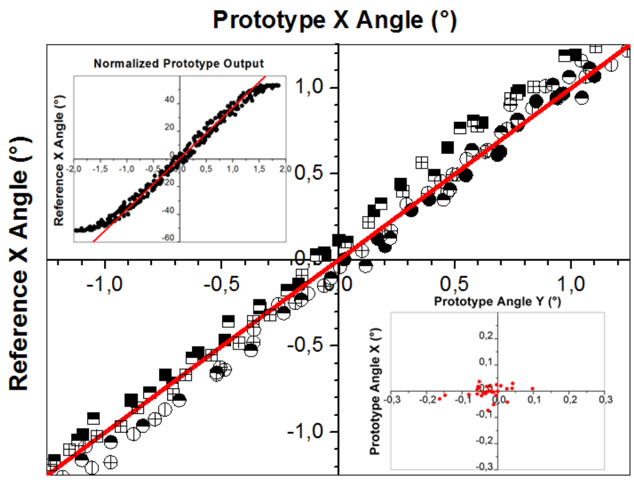

Figure 6: Experimental results of the structured membrane. Main graph: Plot showing significant hysteresis effects of prototype inclinometer measurements over the ±1° linear range (ascending sweeps with circles, descending with rectangles). Top left Inset: Full range normalized prototype output in x-direction. Linear fit to obtain calibration coefficient of 36,8/°. Bottom right Inset: Repeatability test following large angle tilt (>10°) showing standard deviation: y=0,024°, x =0,051°

CONCLUSION

This paper detailed a low-power bi-axial miniaturized inclinometer displaying linear behavior over a large part of the measurement range, which can be tuned by adapting the membrane diameter and thickness (by controlling etch time, or using a high-precision SOI substrate). The use of high precision balls showed sub-0.05° precision levels, the errors being due to mobile mass surface roughness and sphericity errors. Using a fluidic droplet as mobile mass resulted in even better precision, but introduced hysteresis in the system. Since the membrane deflection is influenced by pressure (equation 1) an external pressure sensor is needed for accurate operation. Future work will include a more in-depth analysis and understanding of underlying physics and better alignment of the optical system with the membrane center through improved packaging in order to develop a sensor combining both high precision and low hysteresis.

ACKNOWLEDGEMENTS

We would like to thank Mr. Eric Laurent, Mr. Gilles Hovhanessian and Mr. Bernard Basile from Advitam for providing general technical assistance and civil engineering expertise, and for supplying reference inclinometers for this study. This work was supported by the Ile de France region through the SIPRIS project.

REFERENCES

[1] L.Tang et al., “MEMS Inclinometer based on a novel piezoresistor structure“, *Microelectronics Journal*, vol. 40, pp.78– 82, 2009

[2] L.Shuangfeng, M.Tiehua, H.Wen, “Design and fabrication of a new miniaturized capacitive accelerometer”, *Sensors and Actuators*, A 147, pp.70–74, 2008

[3] H.Jung, C.Kim, S.Kong, “An optimized MEMS-based electrolytic tilt sensor“, *Sensors and Actuators,* vol. A139, pp.23-30, 2007

[4] B.Ando, S.Baglio, A.Beninato, “A ferrofluid inclinometer with a time domain readout strategy”, Procedia Engineering vol. 47, pp.586 – 589, 2012

[5] J.S.Bajic et al., “A simple, low-cost, high-sensitivity fiber-optic tilt sensor”, *Sensors and Actuators*, vol. A185, pp.33-38, 2012

[6] K.-M. Liao, R.Chen, B.Chou, “A novel thermal-bubble-based micromachined accelerometer”, *Sensors and Actuators,* vol. A130–131, pp.282–289, 2006

[7] T.Constandinou, J.Georgiou, “Micro-Optoelectromechanical Tilt Sensor”, *Journal of Sensors,* Article ID 782764, 2008

[8] H.Kato et al., “Photoelectric inclination sensor and its application to the measurement of the shapes of 3D-objects”, *IEEE Transactions on Instrumentation and Measurement,* vol. 40, pp.1021-1026, 1991

[9] D.Welch, J.Georgiou, J.Christen, “Fully differential current-mode MEMS dual-axis optical inclination sensor”, *Sensors and Actuators,* vol. A192, pp.133-139, 2013

[10] ADIS16209 High accuracy, dual axis digital inclinometer and accelerometer, Analog Devices datasheet, 2012

[11] N.Gaber et al., “On the free-space Gaussian beam coupling to droplet optical resonators”, Lab Chip vol.13, pp.826-833, 2013

[12] W.C.Young, R.G.Budynas, *Roark’s Formulas for Stress and Strain*, McGraw-Hill, 2002

[13] A.G.Striz, S.K..Jang, C.W.Bert, “Nonlinear Bending Analysis of Thin Circular Plates by Differential Quadrature”, *Thin Walled Structures*, vol. 6, pp.51-62, 1988

[14] LSOP/LSOC DC-Operated, Gravity-Referenced Inclinometer, Sherborne Sensors datasheet, 2003